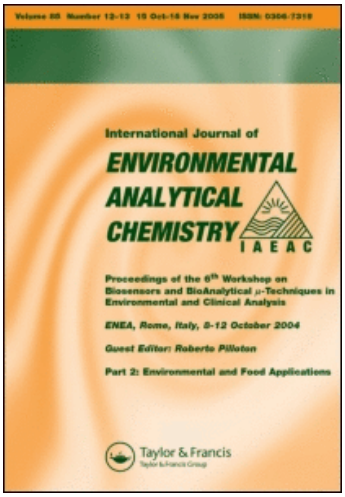

International Journal of Environmental Analytical Chemistry

Publication details, including instructions for authors and subscription information:
http://www.informaworld.com/smpp/title~content=t713640455

Characterization of Size-Fractionated Aerosol from the Jungfraujoch (3580 m asl) Using Total Reflection X-Ray Fluorescence (TXRF)

Niklaus Streit[a]; Ernest Weingartner[a]; Christoph Zellweger[ab]; Margit Schwikowski[a]; Heinz W. Gäggeler[ac]; Urs Baltensperger[a]

[a] Laboratory of Radio- and Environmental Chemistry, Paul Scherrer Institute, Villigen, PSI, Switzerland [b] EMPA, Dübendorf, Switzerland [c] Department of Chemistry and Biochemistry, University of Bern, Bern, Switzerland

To cite this Article Streit, Niklaus , Weingartner, Ernest , Zellweger, Christoph , Schwikowski, Margit , Gäggeler, Heinz W. and Baltensperger, Urs(2000) 'Characterization of Size-Fractionated Aerosol from the Jungfraujoch (3580 m asl) Using Total Reflection X-Ray Fluorescence (TXRF)', International Journal of Environmental Analytical Chemistry, 76: 1, 1 — 16

To link to this Article: DOI: 10.1080/03067310008034114

URL: http://dx.doi.org/10.1080/03067310008034114

Intern. J. Environ. Anal. Chem., Vol. 76(1), pp. 1-16
Reprints available directly from the publisher
Photocopying permitted by license only

CHARACTERIZATION OF SIZE-FRACTIONATED AEROSOL FROM THE JUNGFRAUJOCH (3580 m asl) USING TOTAL REFLECTION X-RAY FLUORESCENCE (TXRF)

NIKLAUS STREIT[a], ERNEST WEINGARTNER[a], CHRISTOPH ZELLWEGER[ab], MARGIT SCHWIKOWSKI[a], HEINZ W. GÄGGELER[ac] and URS BALTENSPERGER[a*]

[a]Laboratory of Radio- and Environmental Chemistry, Paul Scherrer Institute, CH-5232 Villigen PSI, Switzerland, [b]EMPA, CH-8600 Dübendorf, Switzerland and [c]Department of Chemistry and Biochemistry, University of Bern, CH-3012 Bern, Switzerland

(Received 23 April, 1999; In final form 20 July, 1999)

During three field campaigns at the Jungfraujoch High Alpine Research Station, Switzerland, size-fractionated aerosol was collected using a cascade impactor. The particles were impacted on silicon oil-coated quartz sampling substrates. The actual analysis was then performed directly on these quartz sampling substrates using total reflection X-ray fluorescence. The resulting size distributions of 16 elements (S, Cl, K, Ca, Ti, Mn, Fe, Cu, Zn, Se, Br, Rb, Sr, Y, Zr, Pb) were investigated to determine the best cut-off diameter to distinguish between geogenic and anthropogenic particles. The obtained cut-off diameter of 1 μm is an important parameter in the current world-wide measurements under the auspices of the World Meteorological Organization's Global Atmosphere Watch aerosol project.

Keywords: Aerosol; impactor; total reflection X-ray fluorescence (TXRF); size distribution

INTRODUCTION

Global climate modeling has made much progress over the last few years. Decades of measurement have provided us with high quality data on greenhouse gases. Despite these advances, there still remains a lot of uncertainty about the global-mean radiative forcing. Much of this uncertainty is due to the poorly quantified influence of tropospheric aerosol on climate change.[1,2,3] As continuous aerosol data are sparse, there is a need for intensified research and monitoring.

* Corresponding author. Fax: +41 56 3104435. E-mail: baltensperger@psi.ch.

Research focuses on both direct and indirect effects of aerosol on climate. Direct effects refer to the scattering of light by particles, which enhances the earth's albedo. Indirect effects base on the fact that particles can serve as cloud condensation nuclei. An increased number of particles presumably leads to a higher concentration of cloud droplets of smaller size and thus an increased cloud albedo.[4] Furthermore, the reduced droplet size probably results in a longer lifetime of the cloud. The sum of these effects is possibly of the same order of magnitude as the effects of greenhouse gases, but of opposite sign.[5] For a single location, this would not necessarily mean a zero net effect, as there are larger gradients in aerosol than in gas concentrations.

The World Meteorological Organization (WMO) has created an aerosol project within its Global Atmosphere Watch (GAW) program[6] to coordinate the assessment of the changes of the atmosphere, including the direct and indirect effect of aerosols on climate, also quantifying the contribution of natural and anthropogenic sources. A world-wide net of global measurement stations is being established, including stations representative of different types of aerosol : clean and polluted continental, marine, arctic, dust, biomass burning, and free troposphere. There are 20 global stations in pristine areas, and about 300 regional stations closer to the source areas.[7] The Jungfraujoch High Alpine Research Station (JFJ, 3580 m asl) has been selected as part of a virtual global GAW station for clean continental air also comprising Zugspitze (2962 m asl, Germany) and Sonnblick (3106 m asl, Austria).

In this program, the following aerosol parameters are to be measured on a continuous basis at the JFJ : optical depth, number concentration of aerosols, mass concentration and chemical composition in two size classes, light scattering and absorption coefficient, and Fuchs surface area of the particles.[8,9] The two size classes were established in order to differentiate between particles of geogenic and anthropogenic origin. Particles of geogenic origin, occurring in the form of wind-blown dust, tend to be larger than particles of anthropogenic origin formed by gas to particle conversion. Our measurements help in deciding whether the cut-off diameter should be determined individually for every measuring station.

The cut-off diameter separating the two size classes was determined during this study using a PIXE brand cascade impactor with subsequent total reflection X-ray fluorescence (TXRF) analysis of the sampling substrates. The method was described by Schneider[10] and so far applied mostly to marine aerosol,[11] but has also been tested for its suitability for routine investigations.[12] It is the further development of two older techniques, combining the use of an impactor originally built for subsequent proton induced X-ray emission analysis (PIXE), and TXRF, which had before been used to analyze filters after wet chemical workup with nitric acid[13] or water.[14] Earlier measurements at the JFJ had

included only chemical analysis without size information,[15] or covered merely short episodes, such as a 1990 Saharan dust event.[16,17]

EXPERIMENTAL

Measurement location

Ambient air was sampled on top of the High Alpine Research Station (3580 m asl; 46.548 °N, 7.984 °E). The Sphinx Building is located on the main crest of the Bernese Alps, Switzerland. The station participates in the Swiss National Monitoring Network for Air Pollution (NABEL) as well as the Swiss Meteorological Institute (SMI) network, and has been described before.[18]

Measurement periods

The sampling time was about one week. The measurements were performed during three field campaigns of five to six weeks each; each one representative of either summer (6 samples, n=6,), fall (n=5), or winter seasons (n=5). They provide information over a good part of a year's course of size distribution at a remote Alpine site. The exact dates of the field campaigns were July 16- August 25 1997 (summer), October 15- November 19 1997 (fall), and January 19- February 19 1998 (winter).

Sampling instrumentation

The inlet used was developed at our institute.[19] As the JFJ station is in clouds 37 % of the time,[20] the inlet is kept at a constant temperature of 10 °C. Other than drying the aerosol and cloud droplets, this also prevents the inlet from freezing over under the harsh weather conditions. It is designed such that cloud droplets smaller than 40 μm are still sampled up to a wind speed of 20 ms^{-1}. The aerosol is aspirated into the building and collected in an impactor. Gravitational settling losses before the impactor are calculated to be less than 10 % for particles smaller than 10 μm. Therefore no correction for losses was applied in this study.

Simple impactors separate particles into two size classes.[21] Cascade impactors have several stages, rendering possible size segregation of particles into more than two classes.[22] They have been used to collect particulate environmental air pollutants for a long time.[23]

A nine stage single-jet low pressure cascade impactor (PIXE I-1L)[24,25] was used here to separate the aerosol particle sizes. The circular impactor is made of electrically conducting molded plastic (carbon-filled polysulfone) to reduce wall losses by electrostatic deposition. In addition, plastic impactors are not as likely to show high blanks as stainless steel impactors.[26]

Figure 1 shows a cross-section of one of the nine stages of a PIXE impactor. The main structure is depicted in white, the black circles are an o-seal, the shaded area the quartz plate, sometimes also referred to as sampling substrate. The particles are aspirated from above, enter the stage, pass through the jet and are either impacted on the sampling substrate by inertia or follow the air stream around it to the next stage. The behavior of a particle in an impactor and similar surroundings is described by the aerodynamic diameter (d_a), which is governed by particle size, shape, and density. Per definition a certain aerodynamic diameter indicates that the particle measured behaves like a unit density sphere of the same diameter. In our cascade impactor, particles with a d_a of >16, 16–8, 8–4, 4–2, 2–1, 1–0.5, 0.5–0.25, 0.25–0.12, and 0.12–0.06 μm are separated in the respective stages at 1000 hPa. The flow of 1.04 $lmin^{-1}$ through the impactor was kept stable by its built-in critical orifice and periodically checked with a bubble flow meter. The typical volume of a weekly sample was 10 m^3.

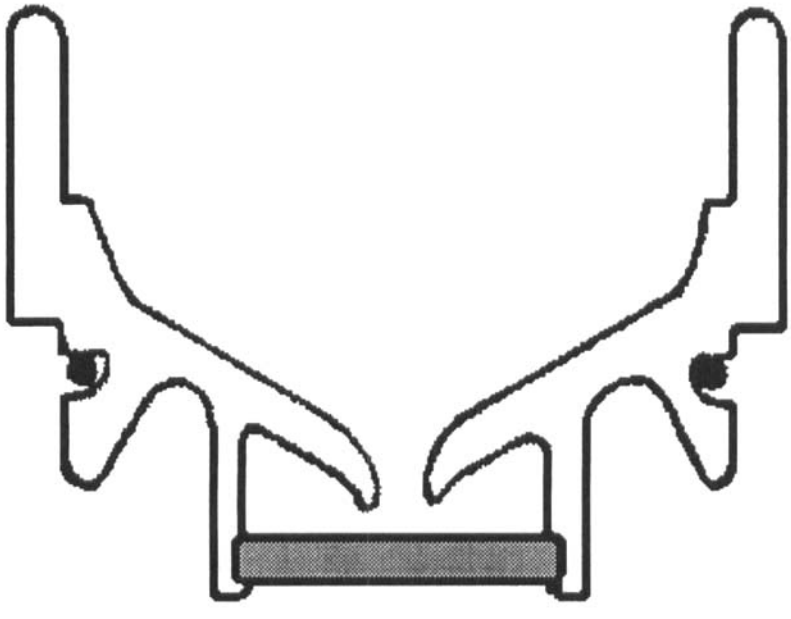

FIGURE 1 One of the nine impactor stages

The quartz plates had been coated with silicon oil to minimize bounce-off of the particles, without significant deterioration of the analysis. The silicon oil used (Merck 109762) had been diluted 1:100 with 2-propanol to facilitate the application of a thin film.

Pressure correction and impactor calibration

The JFJ station lies at an elevation of 3580 m asl where the average ambient pressure is 653 hPa. As the cut-off diameters of the stages are calibrated for an inlet pressure of 1000 hPa, a correction term is necessary in order to compensate for the high altitude of the measuring site. Hillamo et al.[27] have done such pressure correction calculations for the Berner low pressure impactor. We have used their values for the Berner impactor at JFJ conditions[28] for our single-jet impactor without further adjustments.

Table I lists the 50% cut-off diameters (d_{50}) for all stages at sea level and calculations for the JFJ. d_{50} denotes the diameter at which a particle has the same probability of being removed by a stage or passing through it. The expected changes in d_{50} are only significant at the low pressure stages where particles with small aerodynamic diameters are separated.

TABLE I Aerodynamic 50 % cut-off diameters (d_{50}, [μm]) of the PIXE impactor. The two lowest stages (L2, L1) are operated in the low pressure regime

stage	*d_{50} sea level [μm]*	*d_{50} JFJ [μm]*
7	21.9	22.1
6	11.3	11.5
5	5.66	5.66
4	2.82	2.75
3	1.41	1.37
2	0.71	0.69
1	0.35	0.34
L2	0.17	0.17
L1	0.085	0.071

Stahlschmidt et al.[29] have compared the precision of three identical PIXE impactors. They observed similar total lead concentrations, but an internal shift of the size distributions, due to imprecisions in jet and critical orifice diameters. In order to test the accuracy of the PIXE impactor used for our measurements,

monodisperse aerosol was produced at the Jungfraujoch by nebulization and subsequent selection of a narrow size class. The instrumental setup is shown in Figure 2 and explained below.

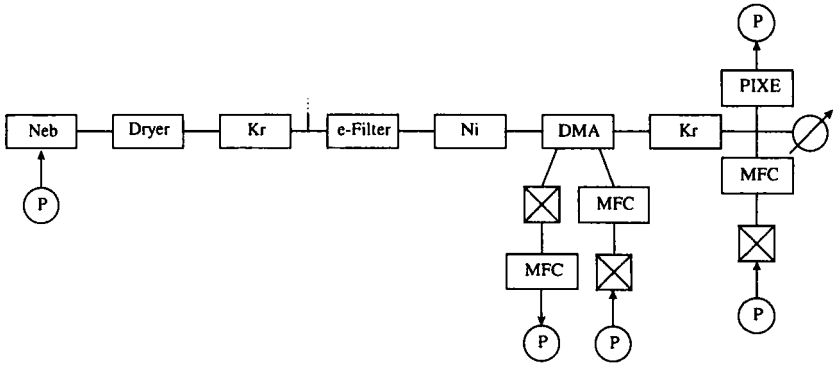

FIGURE 2 Setup of the impactor calibration unit as it was operated on JFJ. (P= pump, Neb= nebulizer, Kr= ^{85}Kr source, e-Filter= electrostatic filter, Ni= ^{63}Ni source, DMA= TSI differential mobility analyzer tube, MFC= mass flow controller, crossed square= particle filter, circle with arrow= pressure meter)

An aqueous solution containing 3 gl^{-1} RbBr (Fluka purum p.a. 83960) was sprayed into the system using a nebulizer (TSI, indicated as Neb on Figure 2). The droplets were dried in a silica gel denuder (dryer) and the aerosol then brought to equilibrium charge by a ^{85}Kr source (Kr, 70 MBq). The charged particles were removed with an electrostatic separator (e-Filter), and some of the remaining particles singly charged by a ^{63}Ni source (Ni, 3 kBq, residence time 20 s). This less ionizing source was chosen to charge particles far below equilibrium and thus to lower the possibility of having multiply charged particles to deal with in the separation step. One distinct size class was then selected in a differential mobility analyzer tube (DMA, TSI 3071) by application of a fixed high voltage equivalent to a single mobility diameter (d_m, with application of a pressure correction for the JFJ).[19] The selected aerosol size class was once again brought to equilibrium charge (Kr, 70 MBq), and the particles were then collected with the PIXE impactor.

RbBr was used as a test aerosol for several reasons. Both elements are suitable for TXRF analysis with Mo excitation, and the salt is soluble in water. It is not abundant, so contamination risks during handling are smaller. Its high density (ρ= 3.35 gcm^{-3}) enabled us to produce particles with large aerodynamic diameters.

In order to facilitate the conversion of the mobility diameters selected by the DMA to the aerodynamic diameters determined by the impactor, a few assumptions were made. As suggested by Kelly and McMurry,[30] the formation of spherical and nonporous particles was assumed, reducing the relationship between aerodynamic (d_a) and mobility diameter (d_m) to

$$d_a = d_m \cdot \sqrt{\rho}.$$

The measured size distributions of two monodisperse aerosols are displayed in Figure 3. They show the Rb concentrations of aerosol particles of 0.85 (left) and 1.6 μm aerodynamic diameter (right) produced at the JFJ with the above setup. It can be seen that the particles are impacted mainly on the expected stages (0.48–0.99 and 0.99–1.9 μm respectively) and that no bouncing is observed.

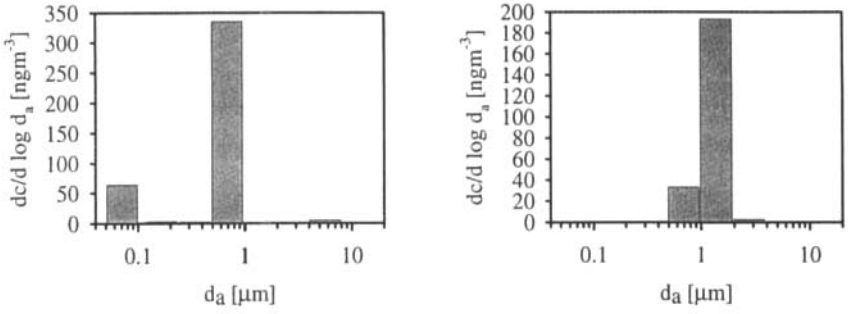

FIGURE 3 Size distributions of aerosol particles of 0.85 (left) and 1.6 μm aerodynamic diameter (right) produced at Jungfraujoch and measured with TXRF. The peak below 0.1 μm on the left is believed to be an artifact

Analytical procedure

Conventional X-ray fluorescence spectra often suffer from high background. The introduction of total reflection X-ray fluorescence was favored by its low background.[31] The method makes use of total reflection at a small irradiation angle, thus reducing scattering on the sampling substrate significantly, leading to lower detection limits. Aiginger and Wobrauschek give an introduction to TXRF[32] and a description of an experimental setup.[33] Prange[34] presents a review of both the TXRF method and its applications, Klockenkämper's textbook[35] gives a thorough treatment of all aspects of TXRF analysis.

Figure 4 shows the setup of the spectrometer used for the analysis.[36] The beam is collimated to 0.05 mm by polished parallel quartz plates and a tungsten slit and then directed at the sampling substrate at an incident angle α of 0.05°.

The instrument depicted was developed and built at the Paul Scherrer Institute.[37] It uses a 2 kW Mo X-ray source operated at 55 kV, a Si(Li) detector and an automated sample loader. The spectra are collected in a multiple channel analyzer (MCA) and the data are treated with Ortec Maestro software.

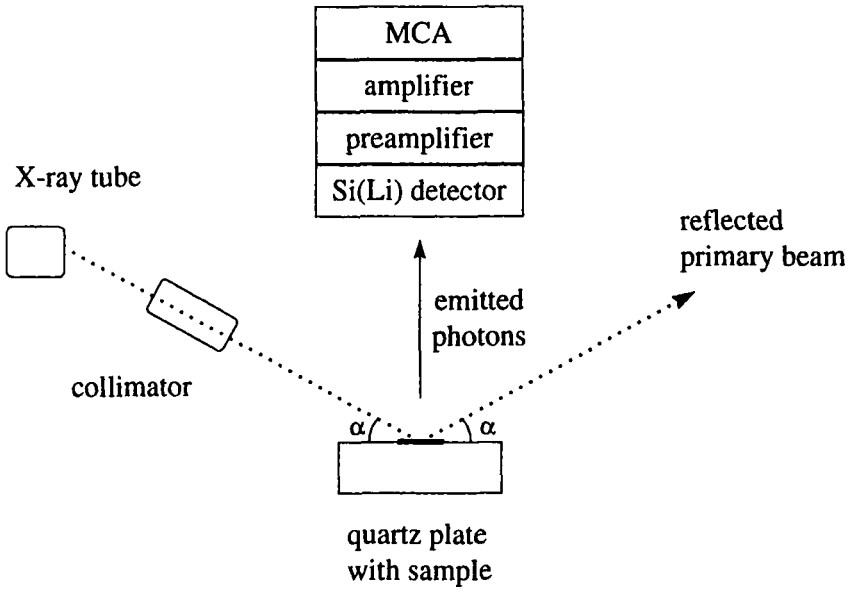

FIGURE 4 Setup of the TXRF spectrometer. The incident angle α of 0.05° is exaggerated in the scheme to facilitate depiction

The space angle covered by the detector was tested by analyzing an array of single element standards placed in increasing distance from the center of the impaction plate. The area covered by the detector exceeded the area of the sample spot by far.

Chemical analysis by total reflection X-ray fluorescence (TXRF) was performed directly on the quartz plates. A total number of 16 weekly sets, each containing nine samples and a blank, were analyzed during 10^4 s (live time) each. Co was used as an internal standard because of its low concentration in high alpine aerosols. 2 μl of a solution containing 40 ng Co were added to the particle spots on the sampling substrates. The water was evaporated and the sample analyzed by TXRF.

The minimum detection limit that can be reached by the PSI TXRF system using Mo excitation is indicated as 3σ values of the method blank. The detection limit is

highest for S (25 ng), decreasing monotonically with increasing atomic number to a minimum for Rb (5 pg), and increasing thereafter. The reason for this behavior is the dependency of the fluorescence cross section on atomic number.

RESULTS AND DISCUSSION

Seasonal variations in the concentrations

Up to 16 elements, i.e. S, Cl, K, Ca, Ti, Mn, Fe, Cu, Zn, Se, Br, Rb, Sr, Y, Zr, and Pb were measured in the samples. The average concentrations of the elements in the air are listed in Table II for summer, fall and winter. The total concentrations were calculated by adding up the concentrations determined on each stage. The mass of the very small particles not retained in the impactor ($d_a < 0.06$ μm) was neglected.

TABLE II The total aerosol element concentrations at Jungfraujoch for the summer, fall and winter field campaigns

element	*concentration in the air [ngm^{-3}]*			*summer/fall ratio*	*summer/winter ratio*
	summer	*fall*	*winter*		
S	107	21	12	5.1	8.9
Cl	6.2	2.3	1.5	2.7	4.1
K	17	3.1	2.4	5.3	6.9
Ca	37	4.1	5.3	9.0	7.0
Ti	3.3	0.35	0.49	9.4	6.8
Mn	0.37	0.24	0.19	1.6	2.0
Fe	26	2.8	5.5	9.5	4.8
Cu	0.49	0.13	0.11	3.8	4.5
Zn	16	2.8	0.59	5.6	27
Se	0.027	0.002	0.001	11	27
Br	0.19	0.049	0.024	4.0	8.0
Rb	0.038	0.007	0.006	5.7	6.8
Sr	0.18	0.024	0.024	7.4	7.4
Y	0.056	0.007	0.003	7.9	19
Zr	0.085	0.005	0.011	17	8.1
Pb	5.4	0.72	0.23	7.5	23

The summer to fall and summer to winter ratios are also indicated in Table II. They show a significant decrease in aerosol concentrations from summer to fall. On the average, the mass decreases by a factor of about six from summer to fall. From

summer to winter, the mass shows an even larger decrease by a factor of about ten. This is mainly due to lower convective transport in fall and winter.[38] Dams and de Jonge[15] who measured several elements at JFJ without size-fractionation also observed a seasonality with the highest concentrations in summer as did Nyeki et al.[39] for a variety of climatically relevant aerosol parameters as well as for the number concentration of particles with diameters between 0.1 and 7.5 μm.

Size distribution spectra of various elements

All elements measured show different size distributions. Yet there are some which display similarities. The summer, fall, and winter size distributions of S, K, Ca, Fe, and Br are shown as examples in Figure 5. These elements were selected because they represent geogenic, anthropogenic, or mixed sources. The error bars represent the standard deviations of the concentrations over one season.

Ca and Fe, which are geogenic elements contained in wind-blown dust, show a maximum in the super-micrometer region, as do other elements of similar origin (Ti, Mn, Rb, and Sr). Br on the other hand, a gasoline additive and thus anthropogenic, has its maximum in the sub-micrometer region, as does S. S occurs mostly as ammonium sulfate, which is created in a gas to particle conversion process from SO_2, followed by neutralization of sulfuric acid. K is included as an intermediate example. It does not fit in either of the above categories, which can be explained by the fact that it has at least two different sources, namely wood-burning (small particles) and crustal material or sea salt (large particles).

When trying to make an even finer distinction within the accumulation mode (0.1–1 μm), S and Br show the most interesting behavior. In summer, S has a bimodal size distribution in the accumulation mode which had already been observed in California as early as 1982.[40]A peak broadening coming close to bimodality is observed for Br in summer, but not for other elements or seasons, unlike in a later study by Hering,[41] where it was observed for many species, and even the overall mass. Contrary to the above phenomena, the apparent bimodalities of S, K, Ca and Fe in the super-micrometer range in winter are merely a result of averaging the samples of the five weeks and cannot be seen in the single measurements.

Enrichment of elements relative to the earth's crust

Particles having their origin in soil dust should have a similar composition as the crust. The vast majority of the earth's crust is made up by the three elements O, Si, and Al, accounting for about 82%. These elements are not detected by our

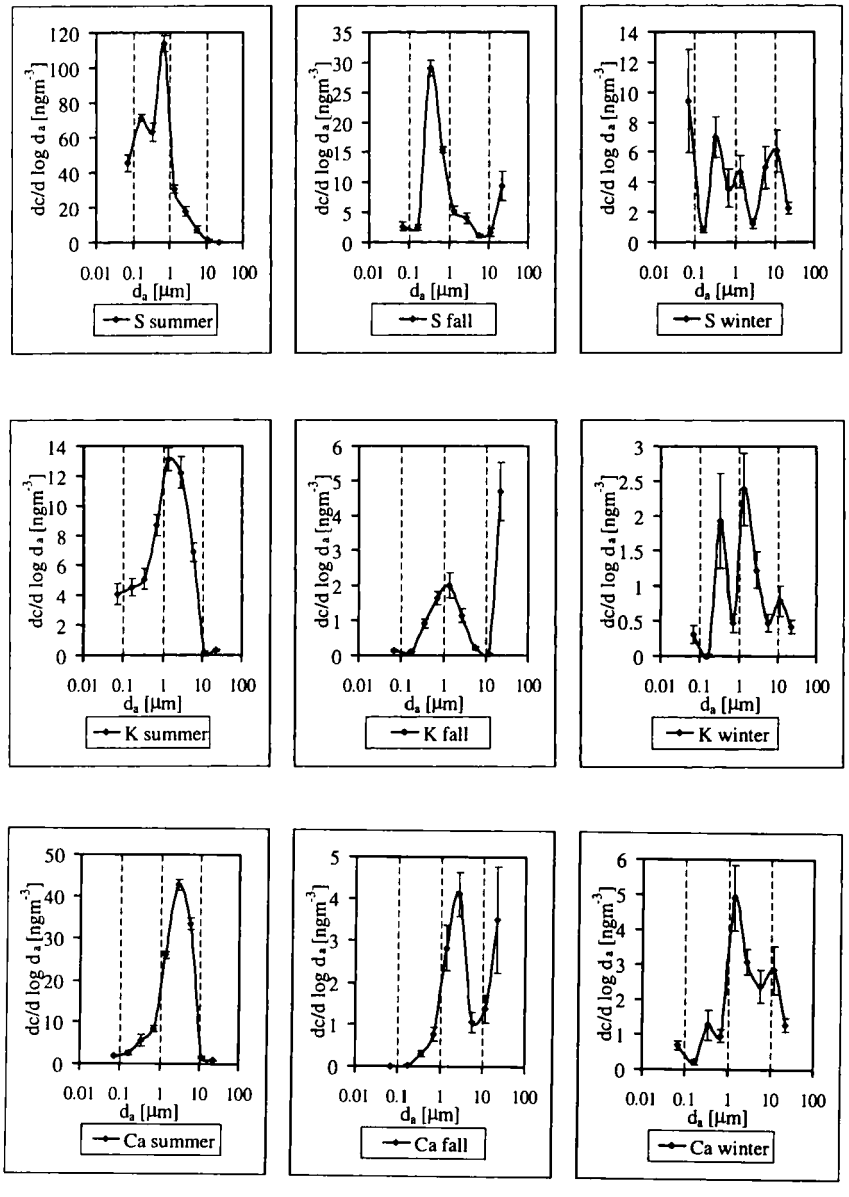

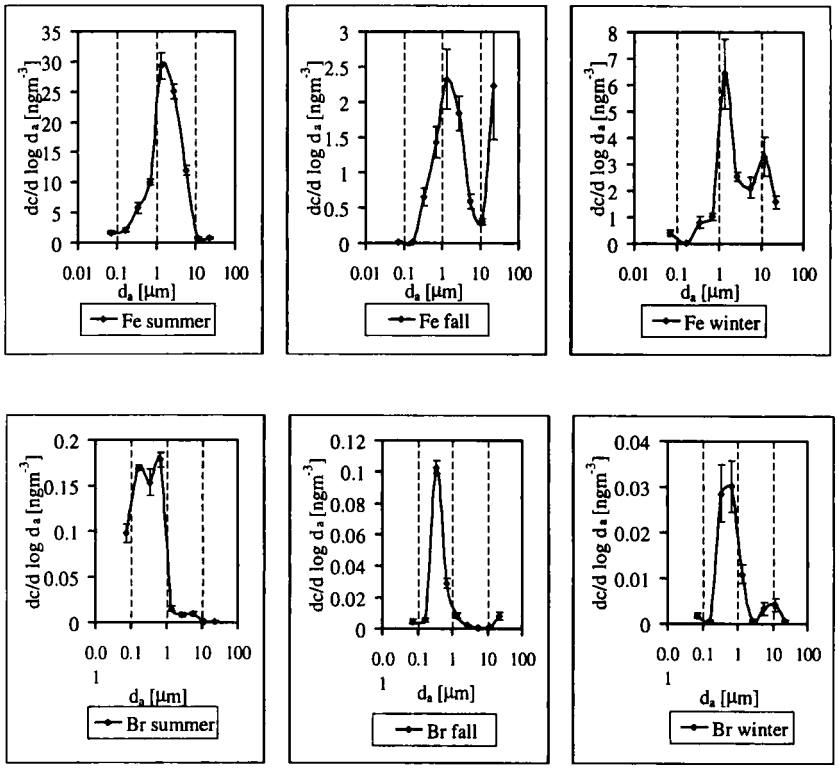

FIGURE 5 The size distributions of S, K, Ca, Fe, and Br (from the top down) at Jungfraujoch during summer (left), fall (center), and winter campaigns (right). The error bars represent the standard deviation of the concentrations over one season (summer n=6 samples, fall n=5, winter n=5)

method. The average concentrations of many of the other elements in the earth's crust[42] and in the aerosol are listed in Table III.

Starting from these values, an enrichment factor (E) can be calculated for each element. Such enrichment factors generally are normalized to the concentration of Al. As our method does not detect Al, Fe was chosen as the reference element to which the others were normalized. As the enrichment behaviors of Fe and Ca resemble each other, Fe seems to be a reasonable choice. The enrichment factors (E) are calculated according to:

$$E = \frac{c(X, aerosol)}{c(X, crust)} \cdot \frac{c(Fe, crust)}{c(Fe, aerosol)}$$

where *c (X, matrix)* denotes the average concentration of the element X in a certain matrix, in our case in the aerosol or the earth's crust.

TABLE III The enrichment factor (E) of elements in aerosols relative to the earth's crust

element	*concentration in the earth's crust [ppm]*[42]	*main mode*	*enrichment (E)*		
			summer	*fall*	*winter*
S	260	fine	780	1500	220
Cl	130	coarse	90	320	76
K	25900		1.2	2.2	0.82
Ca	36300	coarse	1.9	2.0	1.5
Ti	4400	coarse	1.4	1.4	0.92
Mn	950	coarse	0.7	4.5	1.6
Fe	50000	coarse	1.0	1.0	1.0
Cu	55	coarse	17	43	0.70
Zn	70	coarse	430	720	11
Se	0.05		1000	900	170
Br	2.5	fine	150	350	100
Rb	90	coarse	0.8	1.3	0.32
Sr	375	coarse	0.9	1.1	0.60
Y	33	coarse	3.2	3.9	0.86
Zr	165		1.0	0.50	0.53
Pb	13		780	990	120

At first, the enrichments of the elements averaged over all seasons are compared in Figure 6. Zr, Rb, Sr, Ti, K, Ca, Mn, Y, show basically no enrichment compared to the crust. They can be considered to be of geogenic origin. Their size distribution supports the above statement correlating coarse mode and geogenic origin. This does not hold for K, where an anthropogenic contribution is observed in the size distribution. Cl, Br, Zn, Pb, Se, and S on the other hand show a significant enrichment of typically over a factor 100 compared to the earth's crust. They thus clearly have additional, anthropogenic sources. Cu shows an intermediate behavior due to the fact that it has various sources.

The seasonalities of the enrichment factors in Table III are about as expected. Elements of anthropogenic origin show a seasonality, while elements of geogenic origin do not. The enrichment factors of the former are generally higher in summer and fall than in winter. This may be related to the seasonal variation of vertical transport efficiency. Fine mode particles are produced away from the JFJ and thus depend on vertical transport. Coarse particles are produced more locally and do thus not show a seasonality. This is consistent with the findings of Nyeki et al.[39] reporting accumulation to coarse mode volume ratios of ≥ 1.7 in summer and 0.3 in winter.

The enrichment factors are compared with values in ice cores from Colle Gnifetti, Monte Rosa, Switzerland (4450 m asl). Döhring[43] lists the enrichment

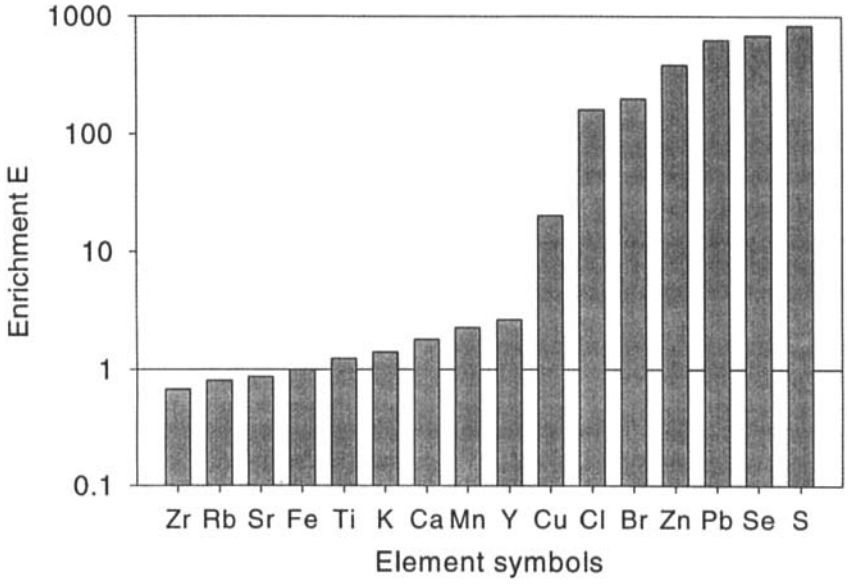

FIGURE 6 The annual averages of the enrichment factors E in increasing order

factors of Ca (E= 1), Cu (17), Zn (41), and Pb (298) for a five-year average up to 1980. Three values compare quite well with the annual averages from this study: Ca (E=1.8), Cu (20), and Pb (630). Only Zn (387) shows a larger difference.

CONCLUSIONS

Following an analysis of up to 16 different elements over two seasons, 1 μm seems to be a reasonable cut-off diameter for the Jungfraujoch station. This criterion will help us to quantify the relative contributions of natural and man-made sources to the High Alpine aerosol after more measurements. These include also other parameters such as volatility, which yields information about the chemical composition, optical properties for the direct effect, and hygroscopicity, influencing both the direct and indirect effect.

Acknowledgements

This study was run under the auspices of the WMO's GAW Project and was in part funded by the SMI. The support of the international foundation of the high-alpine research stations Jungfraujoch and Gornergrat (HFSJG) as well as by

Chr. Widmer for field work, T. Mäkelä and R. E. Hillamo for the pressure correction calculations, and F. Hegedüs of PSI for the TXRF measurements is gratefully acknowledged.

References

[1] J. E. Penner, R. J. Charlson, J. M. Hales, N. S. Laulainen, R. Leifer, T. Novakov, J. Ogren, L. F. Radke, S. E. Schwartz and L. Travis, *Bull. Am. Met. Soc.*, **75**, 375–385 (1994).
[2] S. E. Schwartz and M. O. Andreae, *Science*, **272**, 1121–1122 (1996).
[3] I. Tegen, P. Höllrigl, M. Chin, I. Fung, D. Jacob and J. Penner, *J. Geophys. Res.*, **102**, 23895–23915 (1997).
[4] S. Twomey, *J. Atmos. Sci.*, **34**, 1149–1152, (1977).
[5] Intergovernmental Panel on Climate Change (IPCC), *Climate Change 1994* (J. T. Houghton, L. G. M. Filho, J. Bruce, H. Lee, B. A. Callander, E. Haites, N. Harris and K. Maskell, eds. Cambridge University, Cambridge, 1995), 339 pp.
[6] GAW Technical Fact Sheet No. 12 (WMO, Geneva, 1995), 4 pp.
[7] *The Strategic Plan of the Global Atmosphere Watch (GAW)*, TD 802, (WMO, Geneva, 1997), 83pp.
[8] U. Baltensperger, H. W. Gäggeler, D. T. Jost, M. Lugauer, M. Schwikowski, E. Weingartner and P. Seibert, *J. Geophys. Res.*, **102**, 19707–19719 (1997).
[9] S. Nyeki, U. Baltensperger, I. Colbeck, D. T. Jost, E. Weingartner and H. W. Gäggeler, *J. Geophys. Res.*, **103**, 6097–6107 (1998).
[10] B. Schneider, *Spectrochim. Acta*, **44B**, 519–523 (1989).
[11] T. Stahlschmidt, M. Schulz and W. Dannecker, *Spectrochim. Acta*, **52B**, 995–1001 (1997).
[12] R. Klockenkämper, H. Bayer, A. von Bohlen, M. Schmeling and D. Klockow, *Anal. Sci.*, **11**, 495–498 (1995).
[13] P. Ketelsen and A. Knöchel, *Fresenius Z. Anal. Chem.*, **317**, 333–342 (1984).
[14] D. J. Leland, D. B. Bilbrey, D. E. Leyden, P. Wobrauschek, H. Aiginger and H. Puxbaum, *Anal. Chem.*, **59**, 1911–1914 (1987).
[15] R. Dams and J. de Jonge, *Atmos. Environ.*, **10**, 1079–1084 (1976).
[16] J. Tschiersch, B. Hietel, P. Schramel and F. Trautner, *J. Aerosol Sci.*, **21**, S357-S360 (1990).
[17] M. Schwikowski, P. Seibert, U. Baltensperger and H. W. Gäggeler, *Atmos. Environ.*, **29**, 1829–1842 (1995).
[18] H. Kromp-Kolb, W. Schöner and P. Seibert, *ALPTRAC Data Catalogue* (EUROTRAC International Scientific Secretariat, Garmisch-Partenkirchen, 1993).
[19] E. Weingartner, S. Nyeki and U. Baltensperger, *J. Geophys. Res.*, in press (1999).
[20] U. Baltensperger, M. Schwikowski, D.T. Jost, S. Nyeki, H. W. Gäggeler and O. Poulida, *Atmos. Environ.*, **32**, 3975–3983 (1998).
[21] S. V. Hering, in : *Air Sampling Instruments for Evaluation of Atmospheric Contaminants* (S. V. Hering, ed. ACGIH, Cincinnati, 1989), 7th ed., pp. 337–386.
[22] J. A. Brink, Jr., *Ind. Eng. Chem.*, **50**, 645–648 (1958).
[23] R. I. Mitchell and J. M. Pilcher, *Ind. Eng. Chem.*, **51**, 1039–1042 (1959).
[24] PIXE International Corporation, P. O. Box 2744, Tallahassee, FL 32316, USA.
[25] S. Bauman, P. D. Houmere and J. W. Nelson, *Nucl. Instr. Meth.*, **181**, 499–502 (1981).
[26] M. Schmeling, R. Klockenkämper and D. Klockow, *Spectrochim. Acta*, **52B**, 985–994 (1997).
[27] R. E. Hillamo and E. I. Kauppinen, *Aerosol Sci. Technol.*, **14**, 33–47, (1991).
[28] T. Mäkelä, R. E. Hillamo, personal communication (1999).
[29] T. Stahlschmidt, M. Schulz and W. Dannecker, *J. Aerosol Sci.*, **28**, S115-S116 (1997).
[30] W. P. Kelly and P. H. McMurry, *Aerosol Sci. Technol.*, **17**, 199–212, (1992).
[31] Y. Yoneda and T. Horiuchi, *Rev. Sci. Instrum.*, **42**, 1069–1070 (1971).
[32] H. Aiginger and P. Wobrauschek, in : *Advances in X-ray Analysis* (Plenum, New York, 1985), vol. 28, pp. 1–10.
[33] H. Aiginger and P. Wobrauschek, *Nucl. Instr. Meth.*, **114**, 157–158 (1974).
[34] A. Prange, *Spectrochim. Acta*, **44B**, 437–452 (1989).
[35] R. Klockenkämper, *Total-Reflection X-ray Fluorescence Analysis*, Chemical Analysis vol. 140, (Wiley, New York, 1997), 245 pp.

[36] F. Hegedüs, P. Winkler, P. Wobrauschek and C. Streli, in : *Advances in X-ray Analysis* (C. S. Barrett et al., eds. Plenum, New York, 1990), vol. 33, pp. 581–583.
[37] F. Hegedüs, *Chimia*, **46**, 477–479 (1992).
[38] M. Lugauer, U. Baltensperger, M. Furger, H. W. Gäggeler, D. T. Jost, M. Schwikowski and H. Wanner, *Tellus*, **50B**, 76–92 (1998).
[39] S. Nyeki, F. Li, E. Weingartner, N. Streit, I. Colbeck, H. W. Gäggeler and U. Baltensperger, *J. Geophys. Res.*, **103**, 31749–31761 (1998).
[40] S. V. Hering and S. K. Friedlander, *Atmos. Environ*, **16**. 2647–2656 (1982).
[41] S. Hering, A. Eldering and J. H. Seinfeld, *Atmos. Environ.*, **31**, 1–11(1997).
[42] B. Mason and C. B. Moore, *Principles of Geochemistry*, (Wiley, New York, 1982), 4th. ed., 344 pp.
[43] T. Döhring, Ph.D. thesis, (University of Bern, 1999), 142 pp.